Journal of Hydrology 552 (2017) 660–673

Contents lists available at ScienceDirect

Journal of Hydrology

journal homepage: www.elsevier.com/locate/jhydrol

Research papers

Diffuse nitrogen loss simulation and impact assessment of stereoscopic agriculture pattern by integrated water system model and consideration of multiple existence forms

Yongyong Zhang [a,*], Yang Gao [b], Qiang Yu [c]

[a] Key Laboratory of Water Cycle and Related Land Surface Processes, Institute of Geographic Sciences and Natural Resources Research, Chinese Academy of Sciences, Beijing 100101, China
[b] Key Laboratory of Ecosystem Network Observation and Modeling, Institute of Geographic Sciences and Natural Resources Research, Chinese Academy of Sciences, Beijing 100101, China
[c] School of Life Sciences, Faculty of Science, University of Technology Sydney, PO Box 123, Broadway, NSW 2007, Australia

A R T I C L E I N F O

Article history:
Received 23 May 2017
Received in revised form 13 July 2017
Accepted 14 July 2017
Available online 18 July 2017

Keywords:
Diffuse nitrogen losses
Stereoscopic agriculture
Integrated water system model
Multi-objective calibration
Qianyanzhou station

A B S T R A C T

Agricultural nitrogen loss becomes an increasingly important source of water quality deterioration and eutrophication, even threatens water safety for humanity. Nitrogen dynamic mechanism is still too complicated to be well captured at watershed scale due to its multiple existence forms and instability, disturbance of agricultural management practices. Stereoscopic agriculture is a novel agricultural planting pattern to efficiently use local natural resources (e.g., water, land, sunshine, heat and fertilizer). It is widely promoted as a high yield system and can obtain considerable economic benefits, particularly in China. However, its environmental quality implication is not clear. In our study, Qianyanzhou station is famous for its stereoscopic agriculture pattern of Southern China, and an experimental watershed was selected as our study area. Regional characteristics of runoff and nitrogen losses were simulated by an integrated water system model (HEQM) with multi-objective calibration, and multiple agriculture practices were assessed to find the effective approach for the reduction of diffuse nitrogen losses. Results showed that daily variations of runoff and nitrogen forms were well reproduced throughout watershed, i.e., satisfactory performances for ammonium and nitrate nitrogen (NH_4-N and NO_3-N) loads, good performances for runoff and organic nitrogen (ON) load, and very good performance for total nitrogen (TN) load. The average loss coefficient was 62.74 kg/ha for NH_4-N, 0.98 kg/ha for NO_3-N, 0.0004 kg/ha for ON and 63.80 kg/ha for TN. The dominating form of nitrogen losses was NH_4-N due to the applied fertilizers, and the most dramatic zones aggregated in the middle and downstream regions covered by paddy and orange orchard. In order to control diffuse nitrogen losses, the most effective practices for Qianyanzhou stereoscopic agriculture pattern were to reduce farmland planting scale in the valley by afforestation, particularly for orchard in the downstream regions, followed by fertilizer application optimization.

1. Introduction

Applications of chemical fertilizer and pesticide increase the grain production and improve water use efficiency of crops, which have significantly enhanced global food safety. However, excessive nutrients are washed into water bodies by rainfall runoff, resulting in severe agricultural diffuse pollution. Agricultural nutrient loss is one of the most critical concerns for global freshwater pollution (White et al., 2009). Its proportion of total pollution loads even exceeds that of point source pollution in the USA, the countries in European Union and some developed regions in China (e.g., Yangtze River Delta). For example, agricultural source is estimated to contribute about 65% of the nitrogen loads entering the Gulf from the Mississippi Basin in the USA (Ribaudo et al., 2001), and 60% of the total nitrogen emissions to surface water in the Netherlands (Boers, 1996). The figure is up to 53% of the total nitrogen loads into rivers in China (Ongley et al., 2010), and even reaches 64%, 74% in Tai and Chao Lakes, respectively (Shen et al., 2012). In 2015, the Chinese central government issued an action plan for prevention and control of water pollution, in which, one of ten actions of water pollution is to control agricultural diffuse

* Corresponding author.
E-mail address: zhangyy003@igsnrr.ac.cn (Y. Zhang).

http://dx.doi.org/10.1016/j.jhydrol.2017.07.032
0022-1694/

pollution and to adjust planting structure (State Council of China, 2015). Therefore, it is one of the most critical and urgent tasks to reveal the regional characteristics of agricultural nutrient loss and assess the impact of agricultural practice for environment improvement and sustainable agricultural management.

As one of three basic elements (nitrogen, phosphorus and potassium) of crop nutrients, nitrogen not only plays a very important role in crop growth, but also is a primary element of water pollution. Multiple nitrogen forms exist in crops, soil and water bodies, including ammonium nitrogen (NH_4-N), nitrite nitrogen (NO_2-N), organic nitrogen (ON), nitrate nitrogen (NO_3-N), traces of nitrogen (N_2) and ammonia (NH_3). Interactions and transformations among multiple forms in different media result in the complex mechanism of nitrogen cycling. Modelling approach is a hotspot to integrate multidisciplinary knowledge and skills in hydrology, ecology and agronomy, and to quantify the farmland nitrogen losses at watershed scale. Several representative models have been widely applied, including empirical export coefficient model (Johnes, 1996), process-oriented models based on precipitation-runoff relationship (e.g., AGNPS, ANSWERS, HSPF, SWAT, HBV-N and HYPE) (Young et al., 1987; Bouraoui and Dillaha, 1996; Bicknell et al., 1997; Arheimer and Brandt, 1998; Arnold et al., 1998; Lindström et al., 2010), and biogeochemical models (e.g., SOILN, TEM, DNDC) (Johnsson et al., 1987; Raich et al., 1991; Li et al., 1992). The determination of export coefficients is challenging because the coefficients only reflect conditions at particular sites and are subject to considerable uncertainties through the coefficient transplantation (Ongley et al., 2010). The process-based models focus on the relationship between precipitation and runoff, and link with the nitrogen migration and transformation processes driven by precipitation-runoff erosivity (Zhang et al., 2016). These models, however, are deficient in considering the constraints of other related processes or elements in the nitrogen cycle, such as soil carbon processes, crop physiological and ecological processes (Gassman et al., 2007; Deng et al., 2011). The biogeochemical models have strong advantages in detailing nitrogen processes under the constraints of microbial biomass, carbon pools, water and vegetation uptake in field profiles. Nevertheless, the hydrological migration features at watershed scale are deficient (Deng et al., 2011; Zhang, 2016). Therefore, integration of hydrological and biogeochemical models becomes a popular approach. Some successful cases demonstrate that the simulation performances are improved only for a certain nitrogen forms, such as NO_3-N, NH_4-N (Krysanova et al., 1998; Pohlert et al., 2006; Deng et al., 2011; Zhang, 2016), but the simulation performance of all the nitrogen forms should be tested further.

Stereoscopic agriculture is a novel agricultural development and planting pattern, which has been developed to comprehensively use local natural resources (e.g., land, soil, water, sunshine, heat and biology), and to achieve high efficient agronomic management (e.g., fertilization). This concept was proposed in the beginning of 20th century as the comprehensive management of farming, animal husbandry, processing industry in a certain area (Zhang et al., 2016). It has been widely accepted all over the world as a high-yielding system with multi-functions and layers, and can obtain considerable economic benefits. As a large agricultural country, China also develops three representative stereoscopic agriculture patterns, i.e., fish pond-platform field pattern in the Yellow, Huai and Hai river basins, dike-pond pattern in the Pearl River Delta and Qianyanzhou pattern in the Yangtze river basin (Lu, 1993). Traditional agricultural practice assessment is usually carried out for a single agricultural system to determine effectiveness of different management strategies by using the well-calibrated models mentioned above (Hails, 2002; Krause et al., 2008; Maringanti et al., 2009; Wang et al., 2011). Multiple scenario analysis is usually implemented by designing potential management practices (e.g., fertilizer reduction, land use or cropping pattern changes), and determining the suitable agricultural practices rapidly with the help of human practical experience (Laurent and Ruelland, 2011). However, due to various crops and complicated agricultural managements, studies of impact of the compound system (i.e., stereoscopic agriculture) on diffuse nitrogen losses have still been deficient so far.

In our study, the agricultural diffuse nitrogen losses are simulated with consideration of multiple existence forms by integrated hydrological-biogeochemical model, and the impacts of stereoscopic agriculture are assessed. The main objectives are to: (1) capture the diffuse loss characteristics of different nitrogen forms by integrated water system model (HEQM) with multi-objective calibration in a compound agricultural watershed; (2) identify the critical nitrogen loss regions of current stereoscopic pattern by analyzing the temporal and spatial characteristics of diffuse nitrogen losses; and (3) assess the impact of multiple agricultural practices (fertilization, fallow or afforestation) on diffuse nitrogen losses. All the analysis and results are demonstrated in a small experimental watershed with the representative planting patterns in Southern China. This study is expected to further explore the complicated mechanism of diffuse nitrogen losses, and provide a scientific support for the promotion of stereoscopic agriculture pattern, particularly in China.

2. Material and methods

2.1. Study area and data source

2.1.1. Study area

Qianyanzhou station (115°04′13″E, 26°44′48″N: Fig. 1) is located in Jitai Basin, Taihe County, Jiangxi Province and is one of the basic stations of Chinese Ecosystem Research Network (CERN) (Hao et al., 2017). It is designated as the pilot experimental site of Integrated Scientific Survey in Mountainous-hilly Region of South China, and is the Integrated Development Demonstration Base of stereoscopic agriculture pattern. Qianyanzhou pattern is one of three basic stereoscopic agriculture patterns of China. That is to plant forests and grasses at hilltops, and the fruits and the crops are cultivated at gentle slopes of hillsides or in valleys, while the fish ponds are constructed among the hills.

The station is situated in the northern part of North Sub-tropic zone with red earth hills. The annual mean temperature and precipitation are 17.8° C and 1360 mm. Xiangxi River is one of nine main tributaries in the Qianyanzhou region and its watershed (1.00 km^2) was selected for the assessment of typical stereoscopic agriculture patterns on diffuse nitrogen loss. Terrain declines from the Southwest to the Northeast with elevations from 55 m to 127 m. Main land use types are forest, agricultural land (paddy and dry farmland) and orange orchard, and main soil types are red sandstone and mudstone, which are classified as a mix of oxisol, sand, clay, organic matter, nutrient elements (nitrogen: N, phosphorus: P and potassium: K) and moisture (Gao et al., 2017; Soil Survey Staff, 2010).

2.1.2. Data source

Basic data of Geographic Information System (GIS) was collected from the CERN Synthesis Research Center, including Digital Elevation Model (grid: 20 m × 20 m), rivers, land use (scale: 1:20,000) and soil (scale: 1:20,000). The meteorological data series (daily precipitation, minimum and maximum temperatures) were collected from the weather station in the downstream region.

Three monitoring stations were established along the main stream of Xiangxi River (Table 1). The main land use types varied

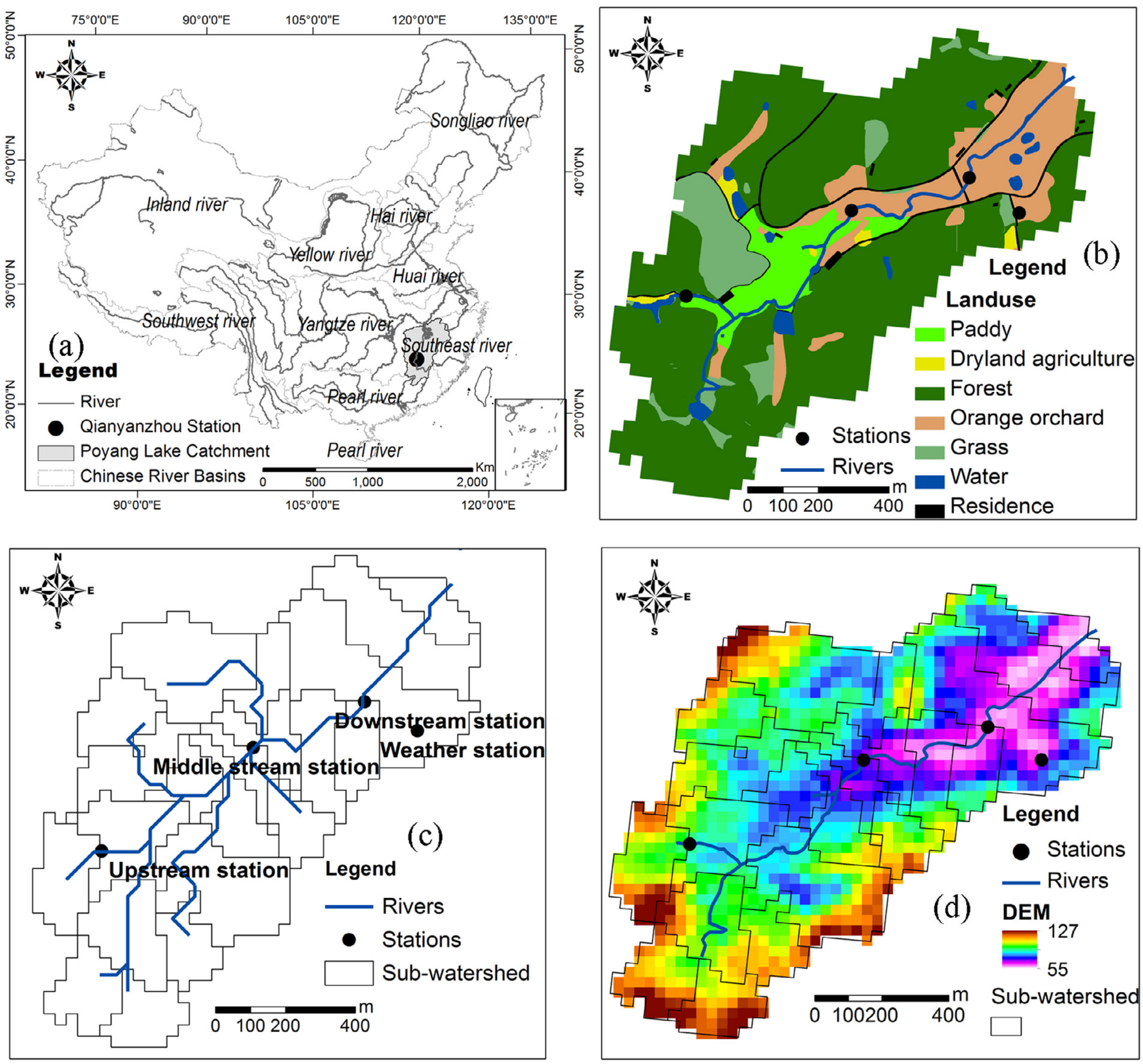

Fig. 1. Location of Qianyanzhou station (a), spatial distribution of land-use (b), sub-watersheds (c) and DEM (d) in the experiment watershed.

Table 1
General characteristics of Xiangxi watershed.

Regions		Upstream	Middle stream	Downstream
Geography	Area (ha)	4.52	50.62	21.87
	Elevation (m a.s.l)	104.77	96.23	84.68
	Mean slope	0.134	0.119	0.131
Land-use/cover (%)	Paddy land	0.60	11.78	2.73
	Dryland agriculture	3.70	0.94	0.06
	Orchard	0.00	5.24	15.65
	Forest	86.86	65.42	73.4
	Grassland	0.98	12.56	3.32
	Water	6.20	2.37	1.80
	Residence	1.66	1.69	3.02
Climate(*)	Precipitation (mm)	1860	1760	1629
	Temperature (°C)	14.6	14.7	14.7

Note: (*) means that the values of precipitations and temperatures are the annual average values from January 1st, 2013 to June 31th, 2016 by using the inverse distance and elevation weighting method (Daly et al., 2002).

throughout the space, i.e., forest, water and dryland agriculture in the upstream region, forest, grass and paddy land in the middle stream region, orchard and paddy land in the downstream region. Water samples were collected at each station twice per month and were taken to the laboratory immediately for water quality test following the national operation standard (SEPA, 2002a). The concentrations of ON, NH_4-N, NO_3-N and TN were measured by a segmented continuous analyzer (Futura, France) after pretreatment.

Moreover, continuous daily runoff was gauged at the downstream station by ISCO 6712 auto samplers (Isco Inc., Lincoln, Nebraska, USA). The monitoring series were from January 1st, 2013 to June 31th, 2016.

Agricultural practice information was investigated from local farmers, including crop types and rotations, sowing and harvest dates, fertilization scheme (rates, dates and types). The main crops were double cropping rice (early rice and late rice) in the paddy land, vegetables (i.e., Chinese cabbage and chili) in the dryland agriculture, and orange in the orchard. The detailed information was shown in Table 1.

2.2. Integrated water system model

2.2.1. Model framework

HEQM is an integrated water system model by coupling multiple water-related processes in hydrology, biogeochemistry, water quality, agriculture crop and interference of human activities (Zhang et al., 2016). The model is proposed for preferable simulations in both hydrological and water quality processes on the hypothesis that the cycles of water and nutrients are inseparable and act as critical linkages among all the coupled water-related processes. Seven major modules are in HEQM, namely hydrological cycle module (HCM), soil biochemical module (SBM), crop growth module (CGM), soil erosion module (SEM), overland water quality module (OQM), water quality module of water bodies (WQM) and dam regulation module (DRM). Moreover, the parameter analysis tool (PAT) is designed for model calibration. The main interactions among the modules, soil and water nitrogen mechanisms are presented in Fig. 2. In particular, Time variant gain model (TVGM: Xia, 1991) is adopted to express the complicated nonlinear relationship between precipitation and runoff (Xia, 1991), and DeNitrification-DeComposition model (DNDC) is adopted to express detailed biogeochemical processes of carbon and nitrogen dynamics in soil layers (Li et al., 1992). The main equations of runoff and nutrient processes were given as follows.

2.2.1.1. Runoff yield. Surface runoff (Rs, mm) is mainly affected by antecedent soil moisture and precipitation (Xia et al., 2005), and interflow (Rss, mm) and baseflow (Rbs, mm) have linear relationships with soil moistures in the upper and lower soil layers, respectively (Wang et al., 2009). The equations are given as

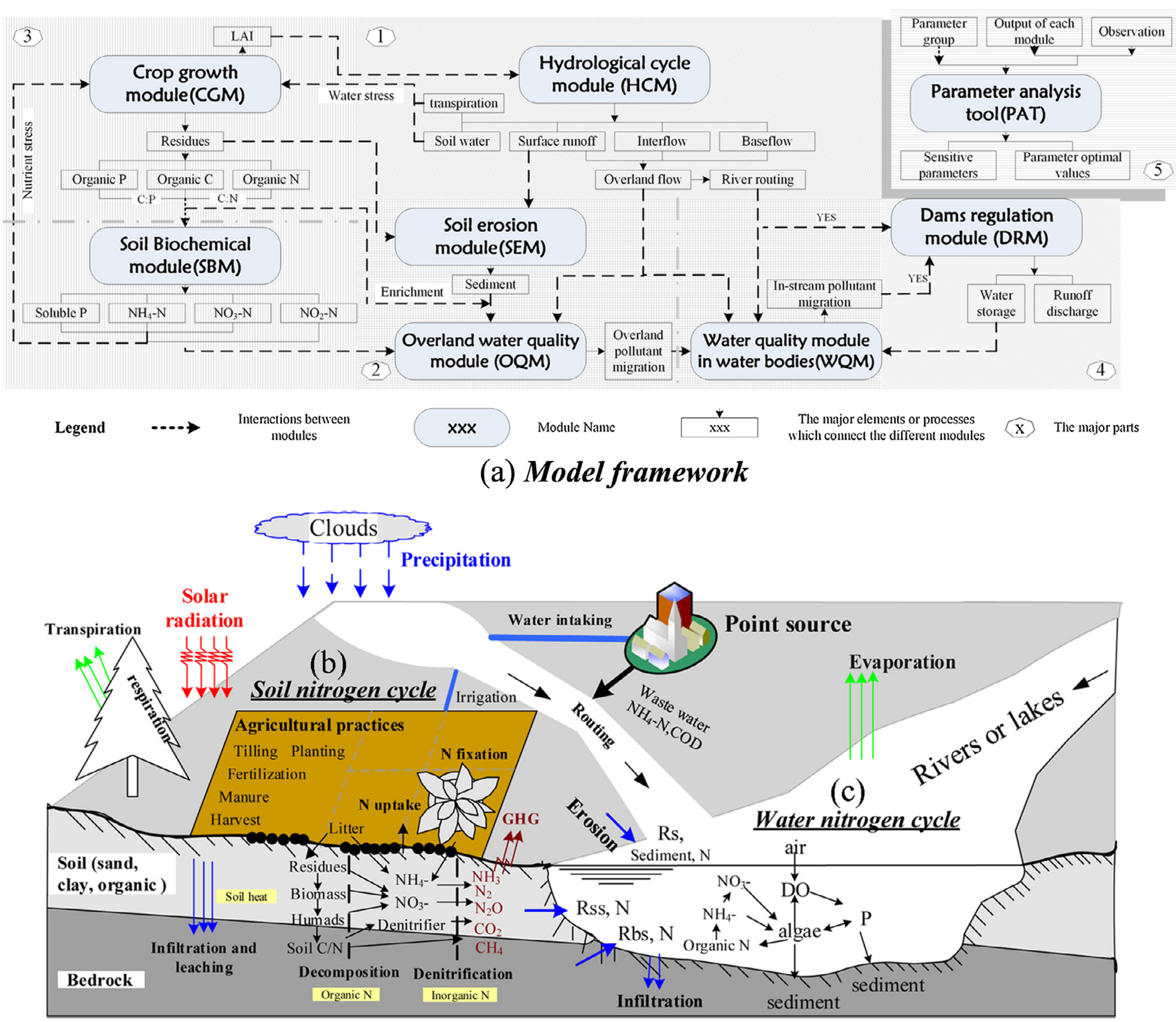

Fig. 2. Main modules of HEQM and their interactions (a), interaction mechanisms of different nitrogen forms in soil (b) and water (c).

$$\begin{cases} Rs = g_1 \cdot (SW_u/W_{sat})^{g_2} \cdot (P\text{- } In) \\ Rss = k_{ss} \cdot SW_u \\ Rbs = k_{bs} \cdot SW_l \end{cases} \quad (1)$$

where SW_u, SW_l and W_{sat} are the soil moistures (mm) in the upper and lower soil layers, and saturation moisture (mm), respectively; the defined depths of the upper and lower soil layers were 1000 mm and 300 mm, respectively in our study; g_1 and g_2 are the basic coefficient of surface runoff, and the influence coefficient of soil moisture, respectively; k_{ss} and k_{bs} are the runoff yield coefficients of interflow and baseflow, respectively; *P* and *In* are the amounts of precipitation and vegetation interception, respectively (mm).

2.2.1.2. Soil nitrogen processes. The main soil nitrogen processes include decomposition (e.g., mineralization, immobilization, NH_3 volatilization and nitrification), denitrification, leaching and loss. The soil decomposition and denitrification processes were considered based on DNDC (Li et al., 1992). For the soil nitrogen decomposition, the accumulated NH_3 volatilization (*AM*, mol/cm^2) and the NH_4 amount (FIX_{NH4}, kg/ha) absorbed by clay and organic matters are estimated by

$$\begin{cases} AM = 2 \cdot (NH_3) \cdot (D \cdot t/3.14)^{0.5} \\ FIX_{NH_4} = [0.41 - 0.47 \cdot \log(NH_4)] \cdot (CLAY/CLAY_{max}) \\ NH_{3_m} = 10^{\{\log(NH_4) - (\log(K_{NH_4}) - \log(K_{H_2O})) + pH\} \cdot (CLAY/CLAY_{max})} \end{cases} \quad (2)$$

where NH_4 and NH_{3m} are the NH_4^+ and NH_3 concentrations (mol/L) in the liquid phase, respectively; *D* is the NH_3 diffusion coefficients (cm^2/d^2); *CLAY* and $CLAY_{\max}$ are the clay content and its maximum content, respectively; K_{NH4} and K_{H2O} are the dissociation constants for NH_4^+:NH_3 equilibrium and H^+: OH^- equilibrium, respectively; *t* is the time step (*s*) and *pH* is the soil pH value.

The nitrification rate (*dNNO*, kg/ha/day) is a function of the available NH_4^+, soil temperature (*T*, °C) and moisture; N_2O emission is a function of soil temperature and soil NH_4^+ concentration, and the equations are given as

$$\begin{cases} dNNO = NH_4 \cdot [1 - \exp(-K_{35} \cdot \mu_{t,n} \cdot dt)] \cdot \mu_{SW,n} \\ N_2O = (0.0014 \cdot NH_4/30.0) \cdot (0.54 + 0.51 \cdot T)/15.8 \end{cases} \quad (3)$$

where K_{35} is the nitrification rate at 35 °C (mg/kg/ha); $\mu_{t,n}$ and $\mu_{sw,n}$ are the adjusted factors of soil temperature and moisture for nitrification, respectively.

For the soil nitrogen denitrification, the NO_3^-, NO_2^-, NO and N_2O denitrification rates are calculated as

$$\begin{cases} dN_xO_y/dt = (u_{N_xO_y}/Y_{N_xO_y} + M_{N_xO_y} \cdot N_xO_y/N) \cdot B(t) \cdot \mu_{PHN_xO_y} \cdot \mu_{t,dn} \\ u_{N_xO_y} = u_{N_xO_y,max} \cdot (C/K_{C,1/2} + C) \cdot (N_xO_y/K_{N_xO_y,1/2} + N_xO_y) \end{cases} \quad (4)$$

where M_{NxOy} and Y_{NxOy} are the maintenance coefficient (1/h), maximum growth yields of NO_3^-, NO_2^-, NO or N_2O (kg/ha/h), respectively; u_{NxOy} and $u_{NxOy,max}$ are the relative and maximum growth rates of NO_2^-, NO_3^- and N_2O denitrifiers, respectively; *C* and *B* are the carbon and denitrifier biomass (kg); μ_{DN} is the relative growth rate of the denitrifiers. $K_{C,1/2}$ and $K_{NxOy,1/2}$ are the half velocity constants of *C* (kg C/m^3) and N_xO_y (kg N/m^3), respectively; $\mu_{PH,NxOy}$ and $\mu_{t,dn}$ are the reduction factors of soil pH and temperature, respectively.

Total nitrogen assimilation is calculated on the basis of the growth rates of denitrifiers and the C: N ratio ($CNR_{D:\ N}$) in the bacteria, and is given as

$$(dN/dt)_{ass} = (dB/dt)_g \cdot (1/CNR_{D:N}) \quad (5)$$

where $(dN/dt)_{ass}$ and $(dB/dt)_g$ are the nitrogen assimilation (kg N/ha/day) and the growth rates (kg C/ha/day) of denitrifiers, respectively.

The emission rates are the functions of adsorption coefficients of the gases in the soil layers and to the air-filled porosity of the soil, and are given as

$$\begin{cases} P(N_2) = 0.017 + ((0.025 - 0.0013 \cdot AD) \cdot PA \\ P(N_2O) = [30.0 \cdot (0.0006 + 0.0013 \cdot AD) + (0.013 - 0.005 \cdot AD)] \cdot PA \\ P(NO) = 0.5 \cdot [(0.0006 + 0.0013 \cdot AD) + (0.013 - 0.005 \cdot AD) \cdot PA] \end{cases} \quad (6)$$

where $P(N_2)$, $P(NO)$ and $P(N_2O)$ are the emission rates of N_2, NO, N_2O during a day, respectively; *PA* and *AD* are the air-filled fraction of the total porosity and adsorption factor depending on clay content in the soil, respectively.

For the soil nitrate leaching, the NO_3^- leaching rate ($Leach_{NO3}$) is a function of clay content, organic C content and water infiltration (W_{inf}, mm) in the soil layer, and is given as

$$Leach_{NO_3} = W_{inf} \cdot \mu_{CLAY} \cdot \mu_{soc}/SW_u \quad (7)$$

where μ_{CLAY} and μ_{soc} are the influence coefficients of clay content and soil organic C, respectively.

For the nitrogen fixation by crops, the amount ($UN_{l,i}$: kg/ha) of NO_3^- and NH_4^+ uptaken by crops in the *l*th soil layer on the *i*th day is calculated as

$$\begin{cases} UN_{l,i} = min[U_{l,i} \cdot (NO_{3,l,i} + NH_{4,l,i})/SW_{u,i}, c_{NB,i} \cdot B_i] \\ UN_{l,i} = Et_{p,t} \cdot [1 - exp(-\Lambda \cdot Z/RZ)]/[1 - exp(-\Lambda)] \end{cases} \quad (8)$$

where $NO_{3,l,i}$ and $NH_{4,l,i}$ are the NO_3^- and NH_4^+ amounts in the *l*th soil layer on the *i*th day (kg/ha); c_{NB} is the optimal N concentration of the crop (kg/ton); *B* is the daily biomass accumulation (ton/ha), which is calculated from CGM; $U_{l,i}$ is water use (mm/day) in the *l*th soil layer on the *i*th day; *Z* and *RZ* are the soil depth and root zone depth (mm), respectively; Λ is a water use distribution parameter; $Et_{p,i}$ is the plant transpiration on the *i*th day (mm), which is calculated from HCM.

For the soil nitrogen loss, the dissolved nitrogen loss is considered to happen in both upper and lower soil layers, while the insoluble organic nitrogen loss only happens in the surface soil migrated with the sediment. The loss weights of NO_3-N, NH_4-N and ON are estimated by

$$\begin{cases} V_{sed\_ON} = 0.001 \cdot V_{sed} \cdot c_{ON} \cdot ER \\ V_{sol\_N} = W_{N\_up} \cdot \left[1 - exp\left(\frac{R_s + R_{ss}}{SW}\right)\right] + W_{N\_low} \cdot \left[1 - exp\left(\frac{R_{bs}}{SW}\right)\right] \end{cases} \quad (9)$$

where V_{sed_ON} is the loss of organic *N* (kg N/ha); c_{ON} is the insoluble nitrogen concentration in the soil layer (g/m^3); *ER* is enrich ratio; W_{N_up} and W_{N_low} are the dissolved nitrogen weights in the upper and lower soil layers, respectively (kg/ha); V_{soil_N} is the total dissolved nitrogen loss (kg N/ha).

2.2.1.3. Nitrogen transformation in water body. The transformation sequence for nitrogen cycle in degradation is that ON→NH_4-N→NO_2-N→NO_3-N. The degradation load is calculated as follows.

$$\begin{cases} V_{d,orgN} = [R_{d,20,orgN} \cdot C_{orgN} - AI_N \cdot R_{d,20,\text{alg}} \cdot C_{\text{alg}}] \cdot 1.047^{(T_{water}-20)} \\ V_{d,NH_4} = [R_{d,20,NH_4} \cdot C_{NH_4} - R_{d,20,orgN} \cdot C_{orgN} \\ \qquad + AI_N \cdot G_{\text{alg}} \cdot A\_N \cdot C_{\text{alg}}] \cdot 1.047^{(T_{water}-20)} \\ V_{d,NO_2} = [R_{d,20,NO_2} \cdot C_{NO_2} - R_{d,20,NH_4} \cdot C_{NH_4}] \cdot 1.047^{(T_{water}-20)} \\ V_{d,NO_3} = [AI_N \cdot G_{\text{alg}} \cdot (1 - A\_N) \cdot C_{\text{alg}} - R_{d,20,NO_2} \cdot C_{NO_2}] \cdot 1.047^{(T_{water}-20)} \end{cases} \quad (10)$$

where $R_{d,20}$ is the degradation coefficient at 20 °C (day^{-1}); AI_N and *A_N* are the N fraction of algal biomass and the algal preference factor for NH_4-N, respectively; T_{water} is the water temperature (°C); $V_{d,orgN}$, $V_{d,NH4}$, $V_{d,NO2}$ and $V_{d,NO3}$ are the degradation loads of ON, NH_4-N,NO_2-N and NO_3-N (mg/day), respectively; C_{orgN}, C_{NH4},

C_{NO2} and C_{NO3} are the concentrations of ON, NH_4-N,NO_2-N and NO_3-N (mg/L), respectively.

2.2.2. Model setup

Input data of HEQM for the simulation of diffuse nitrogen loss include topography, land use, crop, climate, agricultural practice information, as well as initial values of several state variables (e.g., moisture, contents of organic matter, different forms of N and P, pH in the soil layers, water depth and water quality concentrations in rivers) at the sub-watershed scale. Twenty three sub-watersheds and 118 minimum crop units were delineated using Arc GIS platform according to DEM, the spatial distributions of land use and monitoring stations. The areas of sub-watersheds and crop units ranged from 2.36 ha to 11.40 ha, and from 0.007 ha to 8.37 ha, respectively. Seven main land use types were considered, i.e., paddy, dryland agriculture, orchard, forest, grassland, water and residence area. The sub-watershed attributes (e.g., longitude, latitude, elevation, area, land use/cover areas, slopes and their lengths of both land surface and river) and flow routing relationships between sub-watersheds were obtained during the delineation of sub-watersheds.

Because only one weather station existed in our study area, the inverse distance and elevation weighting method (Daly et al., 2002) was adopted to capture the spatial heterogeneity of climate variables (precipitation, maximum and minimum temperatures) through the watershed. The station series of daily climate observations were spatially interpolated for all sub-watersheds by considering the elevation differences and distances between the sub-watershed center and the station.

The crop rotations and fertilization schemes were considered for each sub-watershed by setting the dates of sowing and harvesting, fertilization times and rates. Two fertilization applications (base and additional fertilization) were considered during the complete growth cycle of a specific crop. The initial contents of organic matter, different forms of N and P, pH in each soil layer were determined by averaging the field measurements (Gao et al., 2017) and the spatial distribution of soil types. The initial values of rest state variables (e.g., soil moisture, water depth and water quality concentrations in rivers) were user-defined, which would approach the actual conditions after the warm-up period.

In addition, the calibration period was set from January 1st, 2013 to December 31th, 2014, in which the first two months (January and February of 2013) were the warm-up period. The validation period was from January 1st, 2015 to June 31th, 2016.

2.2.3. Model calibration and validation

Step-by-step procedure was adopted for the calibrations of hydrological and nitrogen related parameters, i.e., hydrological parameters were calibrated first and then nitrogen related parameters were calibrated by fixing the optimal hydrological parameters. For the calibrations of different nitrogen forms (ON, NH_4-N, NO_3-N and TN), it was very difficult to determine the calibration sequence of these forms due to their complex interaction and transformation relationships. Thus, the multi-objective calibration was adopted in simultaneous considering all the interactive objectives of nitrogen forms. Due to comprehensive structure of HEQM, it was not sensible to calibrate all parameters of hydrological and nitrogen processes, e.g., runoff yield and routing, nitrogen transformation and migration, soil erosion, and crop growth. Nine sensitive hydrological parameters and 35 nitrogen related parameters were selected for calibration by LH-OAT (Latin hypercube one factor at a time) in the PAT (Zhang et al., 2016). The rest of parameters remained unchanged, which were determined by field measurements, watershed characteristics and attributes, or related literatures. For example, the growth parameters of typical crops were determined according to the parameter database of DNDC (Li et al., 1992). SCE-UA, as a robust and widely-used auto-optimization algorithm proposed by Duan et al. (1992), was adopted for the HEQM calibration. The relative error is straightforward and also widely accepted to evaluate the model performance of runoff, water quality variables and others. The objective function for model auto-optimization was formulated as

$$\text{Relative error}: \quad RE = \sum_{i=1}^{N} \frac{|O_i - S_i|}{O_i} \tag{11}$$

where N is the number of the series, O_i and S_i are the ith observed and simulated values, respectively. The objective of optimization is to minimize the RE value and the corresponding values of parameter set will be the optimal values.

For the calibration of hydrological parameters, RE between simulated and observed runoff series was adopted to evaluate the hydrological simulation performance, and the objective function was formulated as

$$\begin{aligned} f_{ob-Q} &= minimize(RE_Q) \\ &\quad subject\ to\ par(Q)_{min} \leqslant par(Q) \leqslant par(Q)_{max} \end{aligned} \tag{12}$$

where $f_{ob\text{-}Q}$ is the objective function of hydrological simulation; RE_Q is the RE of simulated runoff magnitude. $par(Q)$, $par(Q)_{\min}$ and $par(Q)_{\max}$ are the hydrological parameter lists, their minimum and maximum limits, respectively.

For the calibration of nitrogen related parameters, all the REs between simulated and observed nitrogen loads of different forms (ON, NH_4-N, NO_3-N and TN) were adopted. The weighted sum approach of multi-objectives was employed to aggregate all the RE objectives into a single objective, and the objective function was formulated as

$$\begin{aligned} f_{ob-N} &= minimize(RE_{ON}, RE_{NH4}, RE_{NO3}, RE_{TN}) \\ &= minimize(\alpha_{ON} \cdot RE_{ON} + \alpha_{NH4} \cdot RE_{NH4} + \alpha_{NO3} \cdot RE_{NO3} + \alpha_{TN} \cdot RE_{TN}) \\ &\quad subject\ to\ par(N)_{min} \leqslant par(N) \leqslant par(N)_{max} \\ &\quad with\ par(Q) = par(Q)_{opt} \end{aligned} \tag{13}$$

where $f_{ob\text{-}N}$ is the objective function of nitrogen simulation; RE_{ON}, RE_{NH4}, RE_{NO3} and RE_{TN} are the REs of simulated ON, NH_4-N, NO_3-N and TN loads, respectively; $par(Q)_{opt}$ is the optimal hydrological parameter list; $par(N)$, $par(N)_{\min}$ and $par(N)_{\max}$ are the nitrogen related parameter lists, their minimum and maximum limits, respectively; α_{ON}, α_{NH4}, α_{NO3} and α_{TN} are the weights of RE_{ON}, RE_{NH4}, RE_{NO3} and RE_{TN}, respectively, and average weights were set in our study, i.e., 1/4. The calibration was implemented in order, from the upstream station to the downstream station.

Three other criteria were also adopted to evaluate the model performance, including normalized bias ($Nbias$), correlation coefficient (r) and coefficient of efficiency (NS) (Nash and Sutcliffe, 1970). The equations were given as

$$\text{Normalized bias}: \quad Nbias = \frac{\sum_{i=1}^{N}(O_i - S_i)}{\sum_{i=1}^{N} O_i} \tag{14}$$

$$\text{Correlation coefficient}: \quad r = \frac{\sum_{i=1}^{N}(O_i - \overline{O}) \cdot (S_i - \overline{S})}{\sqrt{\sum_{i=1}^{N}(O_i - \overline{O})^2 \cdot \sum_{i=1}^{N}(S_i - \overline{S})^2}} \tag{15}$$

$$\text{Coefficient of efficiency}: \quad NS = 1 - \frac{\sum_{i=1}^{N}(O_i - S_i)^2}{\sum_{i=1}^{N}(O_i - \overline{O})^2} \tag{16}$$

where $\overline{O}$ and $\overline{S}$ are the average observed and simulated values, respectively. The model performances of runoff and different nitrogen forms were divided into the unsatisfactory, satisfactory, good, and very good performance ratings, which were determined according to the standards recommended by Moriasi et al. (2007) (Table 2).

2.3. Agricultural practice scenarios and assessment

Fertilization, crop cultural sequence and land use were three main aspects of agricultural practices contributing diffuse nitrogen losses. Five scenarios were designed to evaluate the load reduction performance of diffuse nitrogen losses in terms of reduction of fertilizer application, farmland fallow and afforestation. The detailed scenarios were presented as follows:

(1) Fertilizer application: all the crops were fertilized twice a year at Qianyanzhou station, and the fertilizer rates and dates were determined by field investigation (Hao et al., 2017). Currently, the total rates were 1050–1350 kg/ha/year for rice, 2812.5–3093.75 kg/ha/year for orange trees, and 750 kg/ha/year for vegetables, which were much greater than the upper limit of international standard (225 kg/ha) (Tang et al., 2012). One scenario was designed for the impact assessment of fertilizer reduction on spatial distribution of diffuse nitrogen losses. Thus, Scenario 1 was for optimal fertilizer application with a total rate of 225 kg/ha/year for rice, 70 kg/ha/year for vegetables, 1416 kg/ha/year for orange trees according to the international standard, fertilizer demand amount of vegetables and orange trees (Qian et al., 2007; Shen and Liu, 2013).
(2) Farmland fallow: Three main farmlands (paddy, dryland and orchard) were considered in HEQM, and the crop cultural sequences were the rotation of early rice and late rice in the paddy land, Chinese cabbage and chili rotation in the dryland, and orange in the orchard. For the impact assessment of different farmland fallows on spatial distribution of diffuse nitrogen losses, three scenarios were designed, i.e., paddy land, dryland and orchard lay fallow without fertilization, respectively (Scenarios 2–4).
(3) Farmland afforestation: All the farmlands were reforested, i.e., paddy, dryland and orchard were converted into forests without fertilizer application. This scenario was designed for the impact assessment of ecological restoration on spatial distribution of diffuse nitrogen losses (Scenario 5).

All the scenarios were applied to the entire watershed individually. The well-calibrated HEQM was driven for each scenario by changing the fertilizer application amount, crop management or land use types. The spatial distributions of different forms of nitrogen loads were obtained and compared with the actual distribution (baseline) to find the critical area of nitrogen loss and the potential efficiency.

3. Results and discussion

3.1. Model calibration and validation

3.1.1. Runoff

In the calibration period, the *RE* between simulated and observed daily runoff series at the downstream station was converged to 0.83 after iterations by SCE-UA optimization. The corresponding *Nbias*, *r* and *NS* were 0.00, 0.89 and 0.78, respectively. The calibration performance was at the very good rating. In the validation period, the *RE*, *Nbias*, *r* and *NS* were 0.56, −0.13, 0.82 and 0.67, respectively. The validation performance was at the good rating. Therefore, the simulated hydrograph matched well with the observed hydrograph in both calibration and validation periods (Fig. 3 and Table 3). The hydrological processes were well captured by HEQM in the Xiangxi watershed.

3.1.2. Different forms of nitrogen loads

At the upstream station, the weighted sum *RE* of simulated NH_4-N, NO_3-N, ON and TN loads was converged to an optimal value (0.60) after iterations in the calibration period. For the simulated NH_4-N load, the optimal *Nbias* (−0.43) and *r* (0.87) were at the unsatisfactory and very good performance ratings, but *NS* was only −0.01, at the unsatisfactory performance rating in the calibration period (Fig. 4a). The performance in the validation period was even worse, except *r* (0.98) at the very good performance rating. For the simulated NO_3-N load, the optimal criteria were at the very good rating for *Nbias* and *r*, and good rating for *NS* in the calibration period, but were all at the unsatisfactory rating in the validation period. For the simulated ON load, most optimal criteria were at the very good performance rating in both the calibration and validation periods, except *NS* (0.69) at the good rating. For the simulated TN load, all the optimal criteria were at the very good performance rating in both the calibration and validation periods. Due to good forest cover in this region (86.86% of total area), only trace nitrogen amounts were enriched and lost by precipitation erosion with the average observations of 0.057 kg/day for NH_4-N load, 0.008 kg/day for NO_3-N load, 0.068 kg/day for ON load and 0.195 kg/day for TN load in the streams. The overestimation and mismatching of peak loads of NH_4-N and NO_3-N resulted in the unsatisfactory performances of *Nbias* and *NS*, but the temporal variation of NH_4-N load was well captured with the *r* values being over 0.85. Moreover, the simulation performances of ON, TN loads were at the very good or good ratings.

At the middle stream station, the weighted sum *RE* of simulated NH_4-N, NO_3-N, ON and TN loads also reached the optimal value

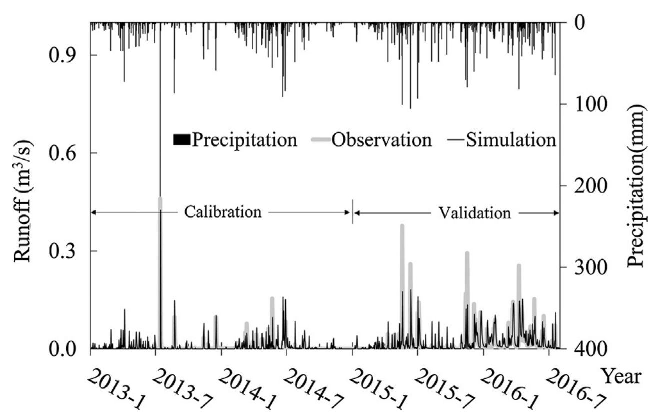

Fig. 3. Simulated and observed daily runoff in the calibration and validation periods at the downstream station.

Table 2
Simulation performance criteria for runoff, different forms of nitrogen loads.

Simulation performance	Nbias		r	NS
	Runoff	Nitrogen load		
Very good	[−0.10,0.10]	[−0.25,0.25]	[0.85,1.00]	[0.75,1.00]
Good	(0.10,0.15] or [−0.15,−0.10)	(0.25,0.40] or [−0.40,0.25)	[0.80,0.85)	[0.60,0.75)
Satisfactory	(0.15,0.25] or [−0.25,−0.15)	(0.40,0.70] or [−0.70,−0.40)	[0.75,0.80)	[0.50,0.60)
Unsatisfactory	(0.25,+∞) or (−∞,−0.25)	(0.70,+∞) or (−∞,−0.70)	(−∞,0.75)	(−∞,0.50)

Table 3
Simulation results of runoff, nitrogen loads (NH_4-N, NO_3-N, ON and TN) from upstream to downstream.

Period		Calibration			Validation		
Stations		Upstream	Middle stream	Downstream	Upstream	Middle stream	Downstream
Runoff	*RE*	–	–	0.83	–	–	0.56
	Nbias	–	–	0.00^{***}	–	–	-0.13^{**}
	r	–	–	0.89^{***}	–	–	0.82^{**}
	NSCE	–	–	0.78^{***}	–	–	0.67^{**}
NH_4-N	*RE*	0.96	0.45	0.34	1.22	0.30	0.53
	Nbias	-0.43^{*}	-0.12^{***}	0.27^{*}	$-1.04^{\#}$	-0.21^{***}	-0.12^{***}
	r	0.87^{***}	0.92^{***}	0.95^{***}	0.98^{***}	1.00^{***}	0.90^{***}
	NS	$-0.01^{\#}$	0.82^{***}	0.88^{***}	$-1.20^{\#}$	0.93^{***}	0.72^{**}
NO_3-N	*RE*	0.56	0.24	0.13	0.98	0.50	0.48
	Nbias	0.23^{***}	-0.16^{***}	-0.05^{***}	$0.98^{\#}$	0.16^{***}	-0.06^{***}
	r	0.85^{***}	0.98^{***}	0.99^{***}	$0.38^{\#}$	0.89^{***}	0.94^{***}
	NS	0.67^{**}	0.96^{***}	0.98^{***}	$-1.16^{\#}$	0.77^{***}	0.74^{**}
ON	*RE*	0.40	0.38	0.40	0.46	0.28	0.48
	Nbias	-0.09^{***}	0.27^{**}	0.37*	0.23^{***}	0.20^{***}	0.44^{*}
	r	0.93^{***}	0.92^{***}	0.92^{***}	0.91^{***}	0.96^{***}	0.90^{***}
	NS	0.82^{***}	0.81^{***}	0.78^{***}	0.69^{**}	0.89^{***}	0.60^{**}
TN	*RE*	0.49	0.57	0.40	0.40	0.41	0.35
	Nbias	-0.21^{***}	−0.28**	-0.20^{***}	-0.01^{***}	-0.23^{***}	-0.15^{***}
	r	0.91^{***}	0.91^{***}	0.93^{***}	0.97^{***}	0.96^{***}	0.99^{***}
	NS	0.80^{***}	0.80^{***}	0.84^{***}	0.84^{***}	0.78^{***}	0.91^{***}

Note: the values with superscripts "#", "*", "**" and "***" represent the results at the unsatisfactory, satisfactory, good, and very good performance ratings, respectively.

(0.41) in the calibration period. All the forms of nitrogen loads were well simulated in both the calibration and validation periods, and all the optimal criteria were at the very good or good ratings (Fig. 4b). At the downstream station, the weighted sum *RE* of simulated NH_4-N, NO_3-N, ON and TN loads was converged to the optimal value (0.32). Most of the optimal criteria were at the very good and good performance ratings, only except some satisfactory ratings for *Nbias* of ON load in the calibration and validation periods (0.37 and 0.44), and NH_4-N load in the calibration period (0.27) (Fig. 4c). In particular, all the *r* and *NS* values were over 0.85 and 0.75, respectively. As the stream flows through the agricultural land and orchard in the middle and downstream regions, all the forms of nitrogen loads increased in the stream and the simulation performances were improved obviously. The average nitrogen loads were increased to 0.990 kg/day for NH_4-N, 0.879 kg/day for NO_3-N, 0.342 kg/day for ON and 3.619 kg/day for TN in the middle stream, and 0.265 kg/day for ON, 0.556 kg/day for NH_4-N, 1.729 kg/day for NO_3-N and 5.443 kg/day for TN in the downstream. Moreover, ON and NH_4-N probably changed to NO_3-N along the streams. In summary, HEQM was also able to well capture diffuse losses and stream dynamic processes of different nitrogen forms, particularly in the agricultural regions.

3.2. Regional distribution of runoff and diffuse nitrogen losses

The runoff coefficients ranged from 0.251 to 0.329 with an average of 0.289 (Fig. 5). The regional distribution of runoff coefficients generally showed a decrease pattern from the upstream region to the downstream region. The great values appeared in the upstream sub-watersheds covered by forest and middle stream sub-watersheds covered by paddy. Despite strong water retention capacity of forest ecosystem, high intensity of precipitation increased the nonlinear gain factor between precipitation and runoff yield (Xia, 1991) resulting in the large runoff coefficients. Moreover, the runoff coefficient in paddy land was usually greater than that of other agricultural lands because of high soil moisture. The small values appeared in the downstream regions covered by orange orchard. The water retention capacity was relatively weak because the forest coverage rate of orange planting practices was much less than that of the natural forest in the upstream regions.

By field investigation, the applied fertilizers were mainly urea and compound fertilizer in our study area, which was easily hydrolyzed into ammonium ion (NH_4^+). Thus, the dominating form of total nitrogen loss was NH_4-N, and the regional distributions of NH_4-N and TN loads were generally consistent (Fig. 5). The annual average coefficients ranged from 0.00 to 207.51 kg/ha with an average of 62.74 kg/ha for NH_4-N, and from 0.00 to 207.84 kg/ha with an average of 63.80 kg/ha for TN. Their regional distributions were just contrary to those of runoff coefficients, and showed increase patterns from the upstream region to the downstream region. The great coefficients were mainly in the downstream region, followed by the middle stream region, and then the upstream region. The coefficient distribution was highly related with the agricultural lands and their fertilizer applications. Although the runoff coefficients were not very large in the downstream region, the fertilizer rate (over 2000 kg/ha) was the largest in all the agricultural lands. The rate was around 900–1200 kg/ha in the paddy land and no fertilizer was applied in the natural forest land in the upstream region.

Small amounts of ON and NO_3-N loads were also lost because of soil background contents, soil nitrogen denitrification and nitrification, vegetation and water. For the ON load, the coefficients were very tiny, which ranged from 0.000 kg/ha to 0.0010 kg/ha with an average of 0.0004 kg/ha. The great coefficients were mainly in the middle stream region, followed by the downstream region. The main explanation was that the denitrification reaction (from NH_4-N to ON) was usually stimulated by denitrifier in the anaerobic condition when the paddy filed was filled with water, or in the high soil moisture condition (Li et al., 1992). For the NO_3-N load, the coefficients ranged from 0.00 kg/ha to 8.04 kg/ha with an average of 0.98 kg/ha. The great coefficients were also mainly in the middle stream region, while the coefficients were close to 0.00 kg/ha in the upstream and downstream regions. The NO_3-N load was probably from the nitrification reaction in the aerobic condition when the rice was ripe or harvested. Therefore, diffuse nitrogen losses were mainly in the downstream and middle stream regions where agricultural activities were centralized. Complex denitrification and nitrification reactions also existed in these regions, particularly in the paddy fields.

Because NH_4-N was the dominating form of TN in Qianyanzhou station, the rest of this study detailedly reported the reduction

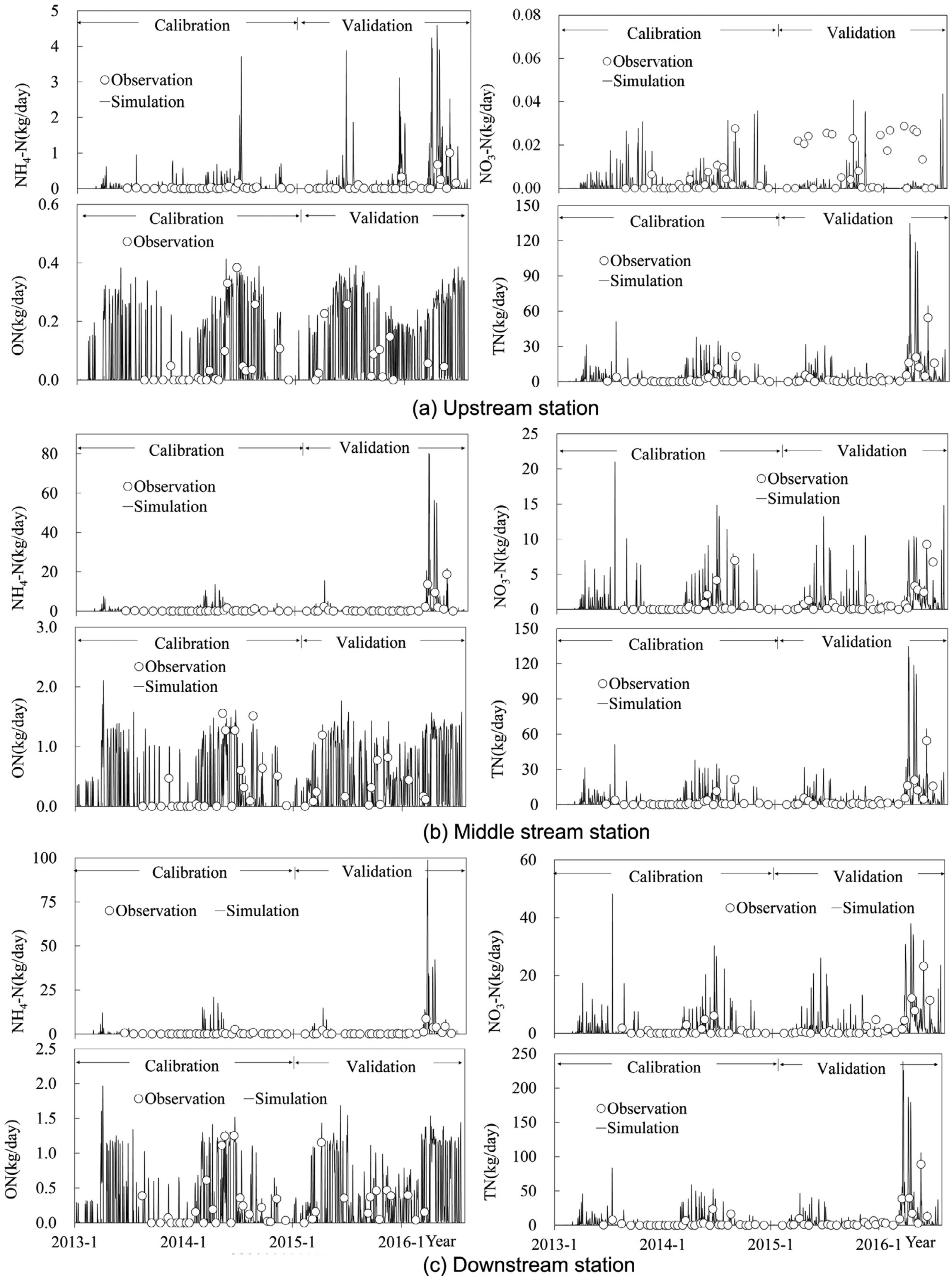

Fig. 4. Simulated and observed daily NH_4-N, NO_3-N, ON and TN in the calibration and validation periods at the upper (a), middle (b) and down (c) stream stations.

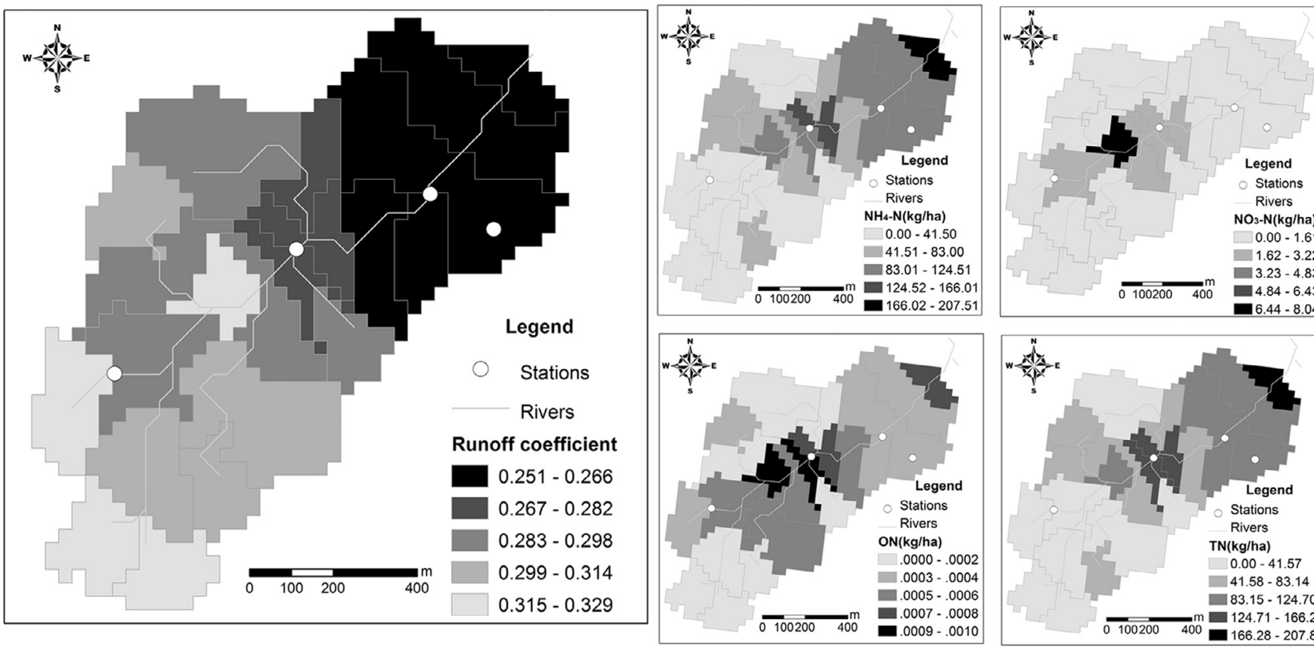

Fig. 5. Regional distributions of runoff coefficients, NH_4-N, NO_3-N, ON and TN loss coefficients for the stereoscopic agriculture.

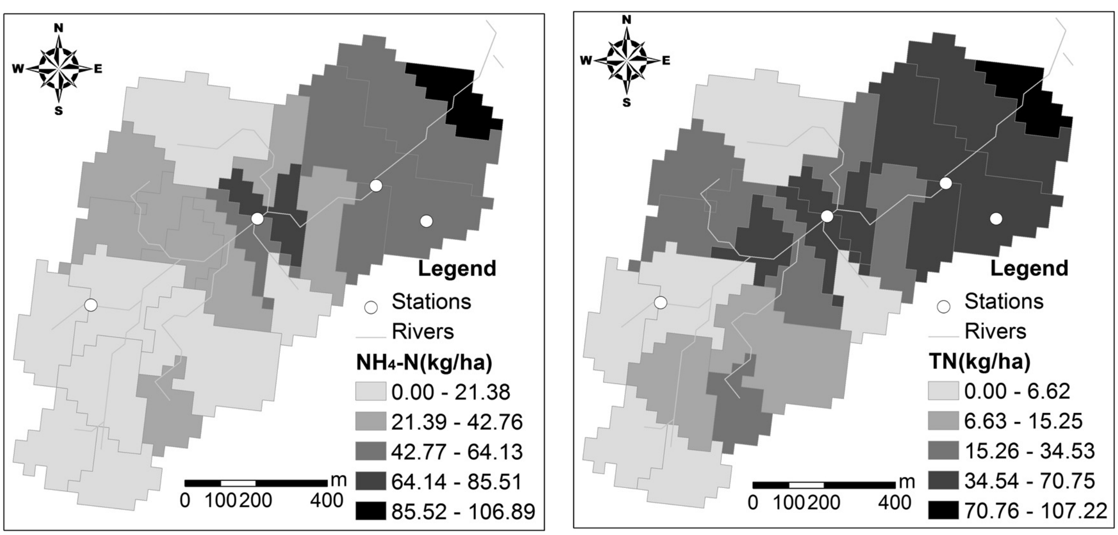

Fig. 6. Regional distributions of NH_4-N and TN loss coefficients for the fertilizer application optimization.

performances of diffuse NH_4-N and TN losses in different agricultural practice scenarios.

3.3. Impact assessment of agricultural practices on diffuse nitrogen losses

3.3.1. Reduction of fertilizer application

Compared with the optimal fertilizer rate, the baseline rate would be reduced by 80% for paddy land, 91% for dryland agriculture and 50% for orange orchard. Accordingly, the diffuse losses of NH_4-N and TN loads were reduced remarkably (Fig. 6). For the NH_4-N load, the coefficients ranged from 0.00 kg/ha to 106.89 kg/ha with an average of 30.68 kg/ha, and the reduction ratios ranged from 0.00 to 64.58% with an average of 43.39%. The most obvious reductions were in the middle stream region with the ratios being over 51.27%, followed by the downstream orchard region with the ratios of nearly 48.00%. The loads were not changed in the upstream region. For the TN load, the loss coefficients ranged from 0.00 kg/ha to 107.22 kg/ha with an average of 31.74 kg/ha, while the reduction ratios ranged from 0.00 to 63.76% with an average of 42.69%. Its regional pattern was quite similar with that of NH_4-N loads because the dominating form of TN was NH_4-N.

3.3.2. Farmland fallow

The paddy land accounted for 6.65% of the total watershed area and was mainly concentrated in the middle valley region. If the paddy land lay fallow, a majority of nitrogen losses were reduced in this region, and no obvious impacts were found in other regions (Fig. 7a). The average NH_4-N coefficient was reduced to 54.63 kg/ha and the reduction ratios in the middle stream region ranged from 16.70% to 96.61%. The average TN coefficient was reduced to 54.71 kg/ha and the reduction ratios in the middle stream region ranged from 18.20% to 95.56%.

The dryland only accounted for 0.68% of the total watershed area and was comparatively distributed near the ponds. If the

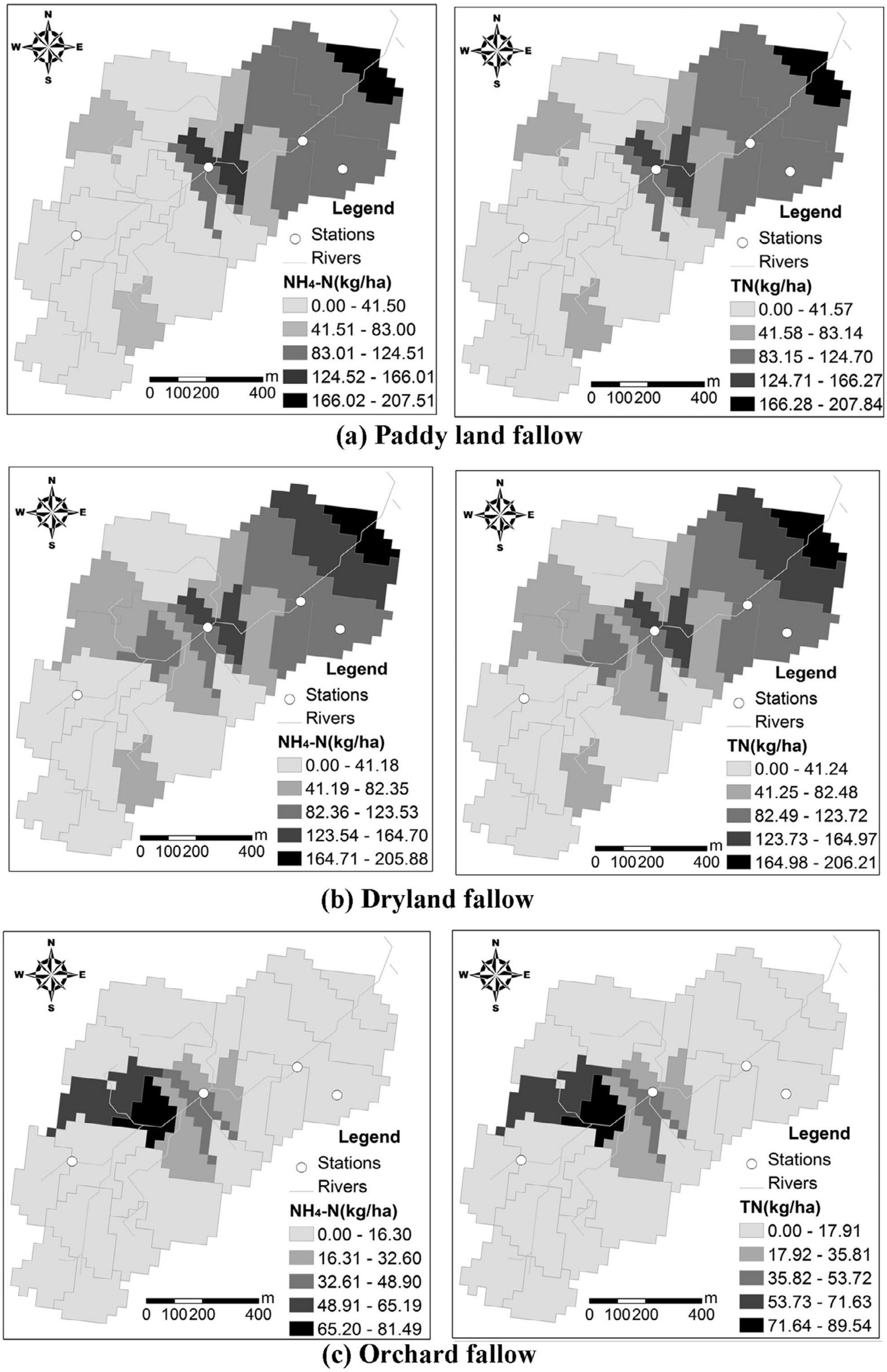

Fig. 7. Regional distributions of NH_4-N and TN loss coefficients for the paddy land (a), dryland (b) and orchard (c) fallow.

dryland lay fallow, the nitrogen losses were reduced in a few regions and the reduction ratios were also quite small (Fig. 7b). The average coefficients of different nitrogen forms were reduced to 60.18 kg/ha with the ratio of 4.08% for NH_4-N loads, and 61.24 kg/ha with the ratio of 4.01% for TN loads.

The orchard accounted for 14.15% of the total watershed area and was mainly concentrated in the middle and downstream valley regions. If the orchard lay fallow, a majority of nitrogen losses were reduced in the middle and downstream regions, and no obvious impacts were found in the upstream region (Fig. 7c). The average NH_4-N coefficient was reduced to 11.76 kg/ha and the reduction ratios ranged from 17.81% to 100% in the most dramatic region. The average TN coefficient was reduced to 12.83 kg/ha and the reduction ratios ranged from 16.47% to 100% in the most dramatic region. Therefore, the most dramatic reductions existed in NH_4-N in the downstream region.

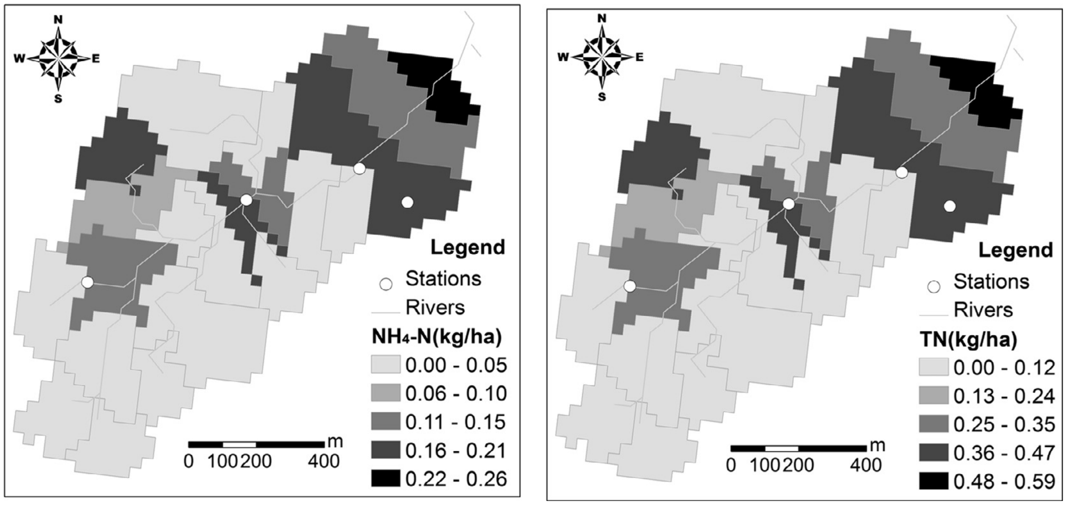

Fig. 8. Regional distributions of NH_4-N and TN loss coefficients for the farmland afforestation.

3.3.3. Farmland afforestation

If all the farmlands (paddy, dryland and orchard) were reforested, the fertilizer applications were halted thoroughly. The diffuse nitrogen losses were reduced drastically throughout the watershed (Fig. 8). The average coefficients of different nitrogen forms were reduced to 0.06 kg/ha with the ratio of 99.90% for NH_4-N loads, 0.14 kg/ha with the ratio of 99.78% for TN loads. Only a tiny of NH_4-N and TN loads were lost to the streams. It can also be deduced that the main TN form was NH_4-N and its source was probably from the atmospheric deposition (Hao et al., 2017). The most dramatic regions were concentrated in the middle and downstream regions covered by paddy and orange orchard.

3.4. Assessment of stereoscopic agriculture

The regional patterns of runoff and nitrogen coefficients showed that the main runoff yield zone was in the upstream region covered by forest with steep terrain, and the main nitrogen loss zone was in the valley along the middle and down streams covered by paddy, dryland and orange orchard. The main source of nitrogen losses was the orange orchard in the downstream region due to its high fertilizer rates and large planting area. In the stereoscopic agriculture of Qianyanzhou station, the runoff yield in the upstream forest region routed into the fish ponds between hills. The slopes were gentle and air temperatures were slightly warm for agricultural planting in the hillsides and valleys (see Table 1). All of these conditions would be advantageous for downstream agricultural irrigation and raising the use efficiency of local water, land and heat resources. However, the water environment condition of middle and down streams would be severely threatened by diffuse nitrogen losses because all the agricultural lands were along the streams and the agricultural pollutant could be easily discharged into the streams. As shown in Fig. 9, the observed NH_4-N concentrations exceeded the slight pollution standard of surface water (GB3838-2002) in the spring and autumn from 2013 to 2016 at the middle and downstream stations. The explanation was that the base fertilizers (urea and compound fertilizer) of rice, vegetables and orange trees were usually applied in the spring and autumn. Additionally, most of TN concentrations even exceeded the high pollution standard at all the three stations. It was probably caused by the fertilizer application and atmospheric nitrogen deposition (Hao et al., 2017).

The effective approaches to controlling diffuse nitrogen losses for Qianyanzhou pattern were to reduce the agricultural fertilizer

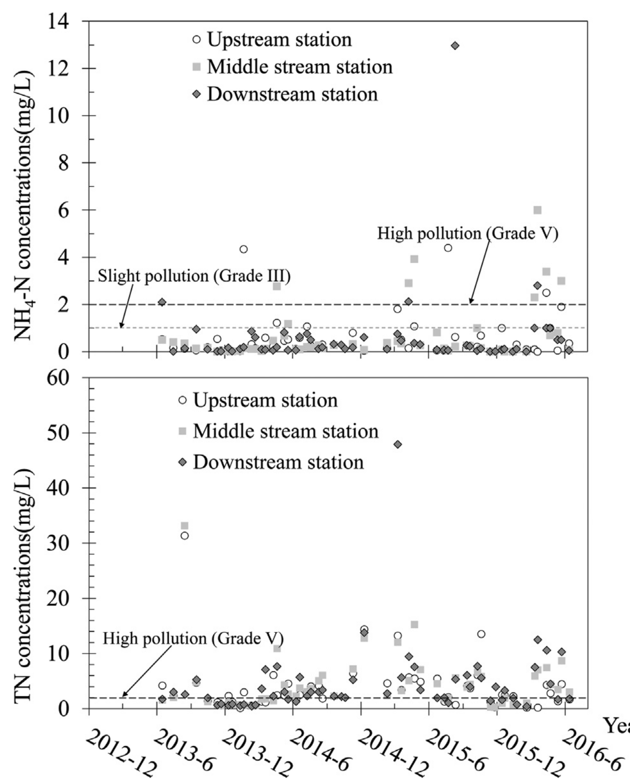

Fig. 9. Observed daily concentrations of NH_4-N and TN at the upper, middle and down stream stations. Note: Grade III means the water quality standard of slight pollution according to SEPA (2002b), e.g., concentrations of NH_4-N and TN are equal to 1.0 mg/L, respectively; Grade V means the water quality standard of high pollution, e.g., concentrations of NH_4-N and TN are equal to 2.0 mg/L, respectively.

application, or reduce the planting scale of orchard by afforestation in the valley. Some auxiliary measures could be adopted, such as vegetation buffer strip along the streams, multi-pond system and wetland system in the streams (Rodriguez et al., 2011).

3.5. Potential uncertainties

Uncertainty issues exist in all environmental modelling. These uncertainties of the diffuse nitrogen simulation, and the impact assessment results of agricultural practices result from simplification of model structure, initial and boundary conditions, as well as equifinality of model parameters (Yang et al., 2008; Li et al., 2010). The parameter sensitivity analysis and autocalibration are very helpful and commonly implemented to reduce the uncertainty sources from integrated water system model (Mantovan and Todini, 2006). Model uncertainties, however, are still inevitable due to high parameterization and complicated interactions among different modules (Zhang et al., 2016). Several statistical techniques should be adopted to quantify the intervals of different uncertainty sources, such as GLUE (Beven and Binley, 1992), Bayesian (Yang et al., 2008), and bootstrap (Shao et al., 2014).

Moreover, the design of multiple potential scenarios also might result in the uncertainties of agricultural practice assessment. In our study, several strategies are adopted. For example, the fertilizer rate is determined according to the international standards (Tang et al., 2012) and field investigation, and the farmland management follows the national policy of land use transitions (e.g., Grain for Green Project) (Lin and Ho, 2003). However, most of these scenarios are to improve the river environment with the sacrifice of economic benefit. This tradeoff issue could be further explored by multiple objective optimization approaches, such as weighted sum approaches (Madsen, 2000), non-dominated evolutionary algorithms (Duan et al., 1992; Deb et al., 2002).

4. Conclusions

Stereoscopic agriculture is a complicated and diverse ecosystem. The environmental quality implications of this agricultural pattern still need to be further investigated due to the multiple existence forms of nitrogen, various features of underlying surface and different management practices. In our study, an integrated water system model (HEQM), multi-objective calibration and scenario analysis were combined to explore the diffuse loss mechanisms of different nitrogen forms, and the effectiveness of agricultural practice in a representative stereoscopic agriculture system of Southern China. Results showed that:

(1) The daily variations of runoff and multiple nitrogen forms were well-reproduced at upper, middle and downstream stations. For the runoff simulation, the *Nbias*, *r* and *NS* were 0.00, 0.89 and 0.78 in the calibration period, and were 0.56, −0.13, 0.82 and 0.67 in the validation period, respectively. For the different nitrogen forms, their simulation performances were mostly at the very good ratings, particularly for the temporal variation with the *r* values of over 0.85. However, the simulation performances of ammonium and nitrate nitrogen were still unsatisfactory at the upstream station because only trace amounts were observed in this region.

(2) For the current stereoscopic agriculture system of Qianyanzhou station, the average annual runoff coefficients ranged from 0.251 to 0.329 with an average of 0.289. The great coefficients were in the upstream region covered by forest with high intensity of precipitation and steep terrain. The nitrogen loss coefficients ranged from 0.000 kg/ha to 0.0010 kg/ha with an average of 0.0004 kg/ha for organic nitrogen, from 0.00 to 207.51 kg/ha with an average of 62.74 kg/ha for ammonium nitrogen, from 0.00 kg/ha to 8.04 kg/ha with an average of 0.98 kg/ha for nitrate nitrogen and from 0.00 to 207.84 kg/ha with an average of 63.80 kg/ha for total nitrogen. Thus, the main form of nitrogen losses was NH_4-N and the most dramatic loss zones were in the middle and downstream regions covered by paddy and orange orchard.

(3) The Qianyanzhou agriculture pattern was advantageous to raise the use efficiency of local water, land and heat resources. However, the water environment condition of middle and down streams was severely threatened by diffuse nitrogen losses because all the agricultural lands were along the streams. Reduction of fertilizer application, farmland fallow and afforestation could reduce the total loads of diffuse nitrogen losses so as to mitigate water quality deterioration. The most effective approach was to reduce the farmland planting scale by afforestation in the valley, particularly for orchard in the downstream regions, followed by the optimization of fertilizer application. The impact of dryland fallow was the least obvious because of its small proportion in the total watershed area.

Acknowledgements

This study was supported by Natural Science Foundation of China (No. 41671024), the China Youth Innovation Promotion Association, Chinese Academy of Sciences (No. 2014041) and the Program for "Bingwei" Excellent Talents in the Institute of Geographic Sciences and Natural Resources Research, Chinese Academy of Sciences (No. 2015RC201). Thanks also to the Editor, Professor Geoff Syme, and two anonymous referees for their constructive comments.

References

Arheimer, B., Brandt, M., 1998. Modelling nitrogen transport and retention in the catchments of southern Sweden. Ambio 27, 471–480.
Arnold, J.G., Srinivasan, R., Muttiah, R.S., Williams, J.R., 1998. Large-area hydrologic modeling and assessment: Part I. Model development. J. Am. Water Resour. Assoc. 34, 73–89.
Beven, K., Binley, A., 1992. The future of distributed models–model calibration and uncertainty prediction. Hydrol. Process. 6 (3), 279–298.
Bicknell, B.R., Imhoff, J.C., Donigian, A.S., Johanson, R.C., 1997. Hydrological simulation program—FORTRAN (HSPF). User's Manual for release 11. EPA—600/R-97/080, 1997. United States Environmental Protection Agency, Athens, GA.
Boers, P.C., 1996. Nutrient emissions from agriculture in the Netherlands, causes and remedies. Water Sci. Technol. 33 (4–5), 183–189.
Bouraoui, F., Dillaha, T.A., 1996. ANSWERS-2000: runoff and sediment transport model. J. Environ. Eng. ASCE 122 (6), 493–502.
Daly, C., Gibson, W.P., Taylor, G.H., Johnson, G.L., Pasteris, P., 2002. A knowledge-based approach to the statistical mapping of climate. Clim. Res. 22, 99–113.
Deb, K., Pratap, A., Agarwal, S., Meyarivan, T., 2002. A fast and elitist multiobjective genetic algorithm: NSGA-II. IEEE Trans. Evolut. Comput. 6 (2), 182–197.
Deng, J., Zhu, B., Zhou, Z.X., Zheng, X.H., Li, C.S., Wang, T., Tang, J.L., 2011. Modeling nitrogen loadings from agricultural soils in southwest China with modified DNDC. J. Geophys. Res. 116, G02020. http://dx.doi.org/10.1029/2010JG001609.
Duan, Q., Sorooshian, S., Gupta, V., 1992. Effective and efficient global optimization for conceptual rainfall-runoff models. Water Resour. Res. 28 (4), 1015–1031.
Gao, Y., Hao, Z., Yang, T.T., He, N.P., Wen, X.F., Yu, G.R., 2017. Effects of atmospheric reactive phosphorus deposition on phosphorus transport in a subtropical watershed: a Chinese case study. Environ. Pollut. 226, 69–78.
Gassman, P.W., Reyes, M.R., Green, C.H., Arnold, A.G., 2007. The soil and water assessment tool: historical development, applications, and future research directions. Trans. ASABE 50, 1211–1250.
Hails, R.S., 2002. Assessing the risks associated with new agricultural practices. Nature 418 (6898), 685–688.
Hao, Z., Gao, Y., Yang, T., Tian, J., 2017. Atmospheric wet deposition of nitrogen in a subtropical watershed in china: characteristics of and impacts on surface water quality. Environ. Sci. Pollut. R. 24 (9), 8489–8503.
Johnes, P.J., 1996. Evaluation and management of the impact of land use change on the nitrogen and phosphorus load delivered to surface waters: the export coefficient modelling approach. J. Hydrol. 183, 323–349.
Johnsson, H., Bergstrom, L., Jansson, P.E., Paustian, K., 1987. Simulated nitrogen dynamics and losses in a layered agricultural soil. Agric. Ecosyst. Environ. 18, 333–356.
Krause, S., Jacobs, J., Voss, A., Bronstert, A., Zehe, E., 2008. Assessing the impact of changes in landuse and management practices on the diffuse pollution and retention of nitrate in a riparian floodplain. Sci. Total Environ. 389, 149–164.
Krysanova, V., Mueller-Wohlfeil, D.I., Becker, A., 1998. Development and test of a spatially distributed hydrological/water quality model for mesoscale watersheds. Ecol. Model. 106, 261–289.

Laurent, F., Ruelland, D., 2011. Assessing impacts of alternative land use and agricultural practices on nitrate pollution at the catchment scale. J. Hydrol. 409 (1–2), 440–450.

Li, C., Frolking, S., Frolking, T.A., 1992. A model of nitrous oxide evolution from soil driven by rainfall events: 1. Model structure and sensitivity. J. Geophys. Res. 97, 9759–9776.

Li, L., Xia, J., Xu, C.-Y., Singh, V.P., 2010. Evaluation of the subjective factors of the GLUE method and comparison with the formal Bayesian method in uncertainty assessment of hydrological models. J. Hydrol. 390 (3–4), 210–221.

Lindström, G., Pers, C.P., Rosberg, R., Strömqvist, J., Arheimer, B., 2010. Development and test of the HYPE (Hydrological Predictions for the Environment) model – a water quality model for different spatial scales. Hydrol. Res. 41, 295–319.

Lin, G.C.S., Ho, S.P.S., 2003. China's land resources and land-use change: Insights from the 1996 land survey. Land Use Policy 20 (2), 87–107.

Lu, L.X., 1993. Chinese Stereoscopic Agriculture Patterns. Henan Science and Technology Press, Zhengzhou, China (In Chinese).

Madsen, H., 2000. Automatic calibration of a conceptual rainfall–runoff model using multiple objectives. J. Hydrol. 235 (3), 276–288.

Mantovan, P., Todini, E., 2006. Hydrological forecasting uncertainty assessment: Incoherence of the GLUE methodology. J. Hydrol. 330, 368–381.

Maringanti, C., Chaubey, I., Popp, J., 2009. Development of a multiobjective optimization tool for the selection and placement of best management practices for nonpoint source pollution control. Water Resour. Res. 45, W06406. http://dx.doi.org/10.1029/2008WR007094.

Moriasi, D.N., Arnold, J.G., Van Liew, M.W., Binger, R.L., Harmel, R.D., Veith, T., 2007. Model evaluation guidelines for systematic quantification of accuracy in watershed simulations. Trans. ASABE 50 (3), 885–900.

Nash, J.E., Sutcliffe, J.V., 1970. River flow forecasting through conceptual models. Part I – A discussion of principles. J. Hydrol. 27, 282–290.

Ongley, E.D., Zhang, X., Yu, T., 2010. Current status of agricultural and rural nonpoint source Pollution assessment in China. Environ. Pollut. 158, 1159–1168.

Pohlert, T., Breuer, L., Huisman, J.A., Frede, H.-G., 2006. Integration of a detailed biogeochemical model into SWAT for improved nitrogen predictions-model development, sensitivity and uncertainty analysis. Ecol. Model. 203, 215–228.

Qian, C.J., Zhu, M.H., Sun, H., Ding, G.Z., 2007. Fertilizer application of common vegetables. Shanghai Vegetables 1, 65–66 (In Chinese).

Raich, J.W., Rastetter, E.B., Melillo, J., Kicklighter, D., Steudler, P.A., Peterson, B.J., Grace, A.L., Moore, B., Vorosmarty, C.J., 1991. Potential net primary productivity in South America: application of a global model. Ecol. Appl. 1, 399–429.

Ribaudo, M.O., Heimlich, R., Claassen, R., Peters, M., 2001. Least-cost management of nonpoint source pollution: source reduction versus interception strategies for controlling nitrogen loss in the Mississippi Basin. Ecol. Econ. 37 (2), 183–197.

Rodriguez, H.G., Popp, J., Maringanti, C., Chaubey, I., 2011. Selection and placement of best management practices used to reduce water quality degradation in Lincoln Lake watershed. Water Resour. Res. 47, W01507. http://dx.doi.org/10.1029/2009WR008549.

Shao, Q., Lerat, J., Podger, G., Dutta, D., 2014. Uncertainty estimation with bias-correction for flow series based on rating curve. J. Hydrol. 510 (3), 137–152.

Shen, Z., Liao, Q., Hong, Q., Gong, Y., 2012. An overview of research on agricultural non-point source pollution modelling in China. Sep. Purif. Technol. 84, 104–111.

Shen, Z.M., Liu, H.D., 2013. Nutrient and Fertilization of Orange Trees. China Agriculture Press, Beijing (In Chinese).

Soil Survey Staff, 2010. Keys to Soil Taxonomy, eleventh ed. United States Department of Agriculture and Natural Resources Conservation Service, Washington, DC, pp. 1–30.

State Council of China, 2015. Action Plan for Prevention and Treatment of Water Pollution. Chinese People's Publishing House, Beijing (In Chinese).

State Environmental Protection Administration of China (SEPA), 2002a. Technical specifications requirements for monitoring of surface water and waste water (HJ-T91-2002) (in Chinese).

State Environmental Protection Administration of China (SEPA), 2002b. Environmental Quality Standards for Surface Water (GB 3838-2002). China Environmental Science Press, Beijing (In Chinese).

Tang, X., Wu, M., Yang, W., Yin, W., Jin, F., Ye, M., Currie, N., Scholz, M., 2012. Ecological strategy for eutrophication control. Water Air Soil Pollut. 223 (2), 723–737.

Xia, J., 1991. Identification of a constrained nonlinear hydrological system described by Volterra Functional Series. Water Resour. Res. 27, 2415–2420.

Xia, J., Wang, G.S., Tan, G., Ye, A.Z., Huang, G.H., 2005. Development of distributed time-variant gain model for nonlinear hydrological systems. Sci. China: Earth Sci. 48, 713–723.

Wang, Y., Tu, C., Cheng, L., Li, C., Gentry, L.F., Hoyt, G.D., Zhang, X., Hu, S., 2011. Long-term impact of farming practices on soil organic carbon and nitrogen pools and microbial biomass and activity. Soil Till. Res. 117, 8–16.

Wang, G., Xia, J., Chen, J., 2009. Quantification of effects of climate variations andhuman activities on runoff by a monthly water balance model: a case study of the Chaobai River basin in northern China. Water Resour. Res. 45. http://dx.doi.org/10.1029/2007WR006768. W00A11.

White, M.J., Storm, D.E., Busteed, P.R., Stoodley, S.H., Phillips, S.J., 2009. Evaluating nonpoint source critical source area contributions at the watershed scale. J. Environ. Qual. 38 (4), 1654–1663.

Yang, J., Reichert, P., Abbaspour, K.C., Xia, J., Yang, H., 2008. Comparing uncertainty analysis techniques for a swat application to the Chaohe basin in China. J. Hydrol. 358 (1), 1–23.

Young, R.A., Onstad, C.A., Bosch, D.D., Anderson, W.P., 1987. AGNPS – a nonpoint-source pollution model for evaluating agricultural watersheds. J. Soil Water Conserv. 44 (2), 169–173.

Zhang, J.F., 2016. Forestry Measures for Ecologically Controlling Non-point Source Pollution in Taihu Lake Watershed, China. Springer, Singapore.

Zhang, Y.Y., Shao, Q.X., Ye, A.Z., Xing, H.T., Xia, J., 2016. Integrated water system simulation by considering hydrological and biogeochemical processes: model development, with parameter sensitivity and autocalibration. Hydrol. Earth Syst. Sci. 20, 529–553.